2R regeneration based on Dispersion-Imbalanced Loop Mirror and its Applications in WDM systems

Chi, Nan; Carlsson, Birger; Jeppesen, Palle

Published in:
Journal of Lightwave Technology

Link to article, DOI:
10.1109/JLT.2002.804032

Publication date:
2002

Document Version
Publisher's PDF, also known as Version of record

2R Regeneration Based on Dispersion-Imbalanced Loop Mirror and Its Applications in WDM Systems

Nan Chi, Birger Carlsson, and Palle Jeppesen, *Member, IEEE*

***Abstract*—2R regeneration based on dispersion -imbalanced loop mirror is investigated including the characteristics of transfer function, output extinction ratio, initial chirp, predispersion, and WDM signals transfer functions. Theoretical results show that the input peak power is a critical parameter for the dispersion-imbalanced loop mirror (DILM) and furthermore, to guarantee the multiwavelength operation of the DILM, limitations due to accumulated dispersion and dispersion slope have to be considered. Our experiment demonstrates that 6×10 Gb/s WDM signals can be successfully regenerated by a novel 2R regenerator based on a DILM consisting of a single mode fiber (SMF) and a highly nonlinear dispersion-shifted fiber (DSF) after WDM transmission over 40 km SMF of the WDM signals.**

***Index Terms*—2R regeneration, dispersion -imbalanced loop mirror (DILM), multiwavelength regenerator, optical fiber dispersion, optical Kerr effect.**

I. Introduction

ULTRAFAST all-optical regeneration techniques are expected to play a major role in future all-optical networks to avoid accumulation of noise, crosstalk, and nonlinear distortions and to ensure good signal quality for transmission [1]. Although at the SDH level, 3R regeneration (Reamplifying, Reshaping, Retiming) could be performed electronically, electronics impose severe technology and economic constrains at data rates near and above 40 Gb/s while all-optical techniques could advantageously remove the electronics bottleneck.

The first R, Reamplification, is achieved by optical amplifiers based on fiber or semiconductor. However, crosstalk is also amplified and noise is added. Hence, a Reshaping element is necessary to suppress noise and crosstalk. The most common scheme is based on a nonlinear optical gate that uses either Kerr effect in optical fiber [2] or active components such as DFB lasers, electroabsorption modulators and semiconductor optical amplifiers (SOAs) [3]–[6]. The scheme based on an electroabsorption modulator with cross-absorption modulation has been tested up to 40 Gb/s [4]. 3R regenerative devices with Mach-Zehnder configuration exploiting cross-phase modulation (XPM) in SOAs have been demonstrated at 40 Gb/s [5], and the ultrafast nonlinear interferometer configuration containing an SOA has allowed 3R regeneration at faster speeds up to 84 Gb/s [6]. For the fiber-based regenerators including the nonlinear optical loop mirror (NOLM) and the dispersion-imbalanced loop mirror (DILM), the operating speed is determined by ultrafast fiber nonlinearity, which provides response times down to a few fs. Though some of these techniques could perform with a tunable wavelength, so far research has focused on single-carrier operation while multiwavelength regeneration, which is a necessity in all-optical WDM systems, has not been demonstrated. However, the DILM that we describe in details in this paper has potential as a multiwavelength regenerator.

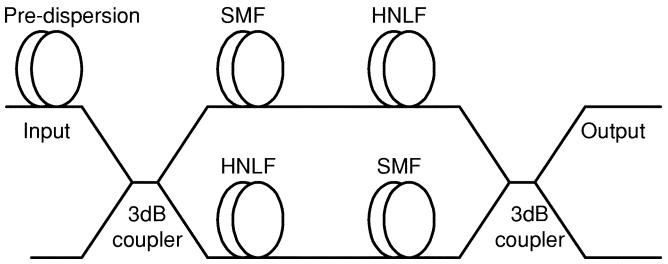

Fig. 1. Equivalent Mach-Zehnder interferometer model.

An asymmetric NOLM can act as a saturable absorber and strong filter in suppressing the amplified spontaneous emission (ASE) noise and reducing the timing jitter and pulse-to-pulse interactions. Unbalancing of the NOLM can be achieved with an asymmetrically placed EDFA close to the loop coupler [7]–[9] or with making the dispersion of the fiber loop asymmetric as so-called DILM. The DILM enables a number of applications such as pulse compression [10], [11], crosstalk suppression in an OTDM system [12], in-band ASE noise filtering [13], self-switching [14] and pedestal suppression in XGM wavelength converters [15]. The 2R regeneration based on DILM works for nonreturn-to-zero (NRZ) and return-to-zero (RZ) format and is bit rate transparent up to the speed limit of the Kerr effect. Theoretical analysis of the switching properties of the DILM described in previous works is based on lumped dispersive elements [16] and only single carrier operation is considered. In this paper, characteristics of the DILM including transmission function, extinction ratio, initial chirp, optimum fiber length, predispersion, and WDM channels operation will all be analyzed in detail.

The paper is organized as follows. The Mach-Zehnder interferometer model for the DILM is presented in Section II. Based on this model, a theoretical analysis is carried out. In Section III, all-optical 2R regeneration of 6×10 Gb/s WDM signals is accomplished experimentally after WDM transmission over 40-km single mode fiber (SMF) by using a novel 2R regenerator based on a DILM consisting of a SMF and a HNLF. Section IV contains a discussion.The clockwise and counter clockwise propagation could be viewed as two arms in an equivalent Mach-Zehnder interferometer as shown in Fig. 1. Before the signal propagates in the interferometer, there is a segment of SMF acting as a predispersion element. Assuming the state of polarization of the two beams is parallel

Manuscript received February 15, 2002; revised July 15, 2002.

The authors are with Research Center COM, Technical University of Denmark, Lyngby DK-2800, Denmark (e-mail:nc@com.dtu.dk).

Digital Object Identifier 10.1109/JLT.2002.804032

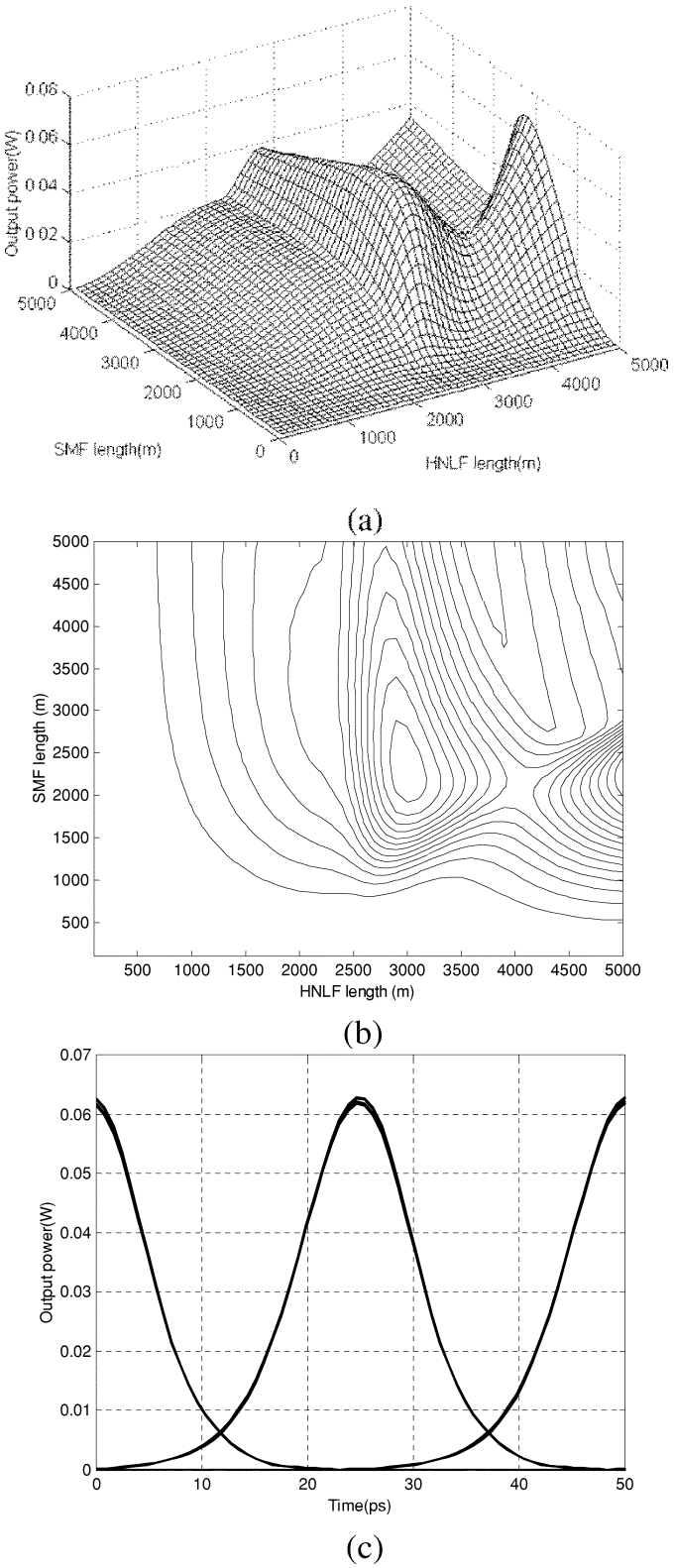

Fig. 2. Output power versus SMF length and HNLF length. (a) Three-dimensional mesh surface. (b) Contour plot. (c) Output eye diagram at the optimum point.

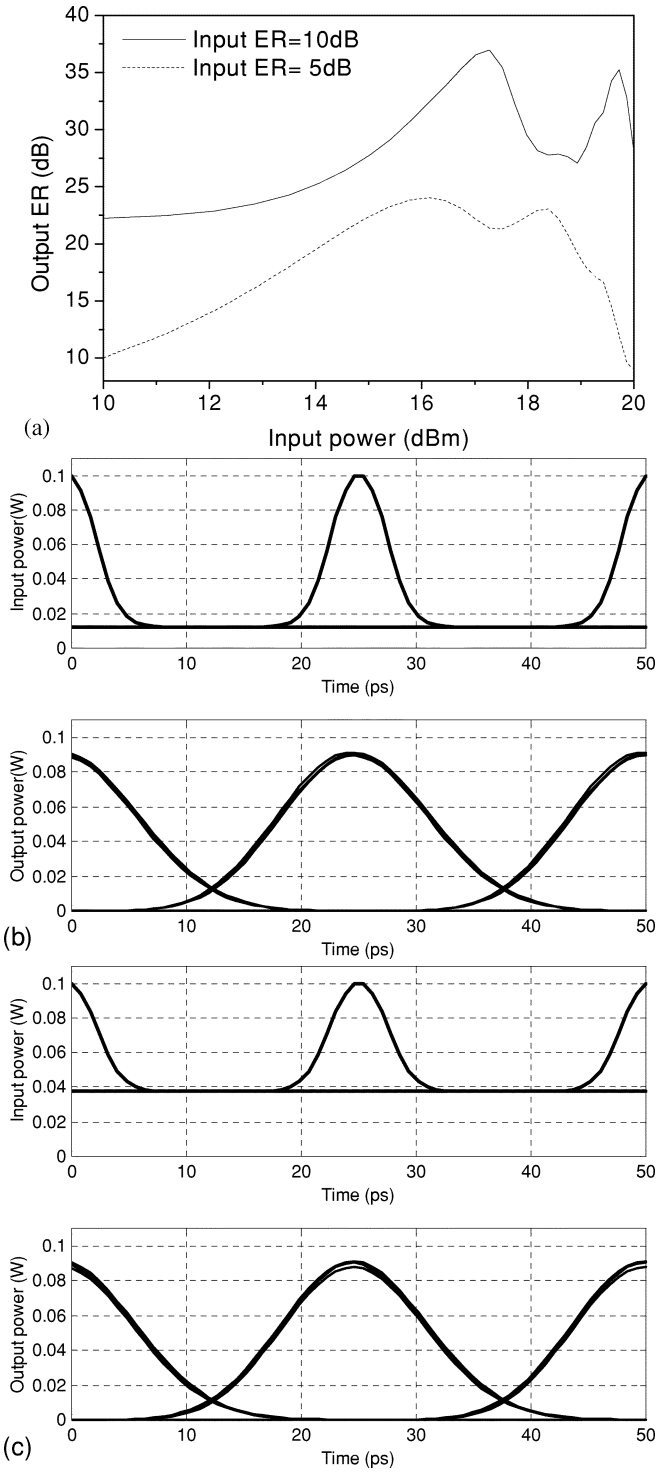

Fig. 3. (a) Output extinction ratio as a function of input average power for two different input extinction ratio levels. (b) Input and output eye diagrams when the input extinction ratio is 10 dB. (c) Input and output eye diagrams when the input extinction ratio is 5 dB.

and the phase shift difference between the two beams is $\Delta\phi$, then the transmission output of the DILM is

$$P_{\text{out}} = |A_1(L,t) - A_2(L,t)|^2 = \frac{(1-\cos\Delta\phi)}{2} P_{\text{in}}. \quad (1)$$

II. Principle and Numerical Simulation

Generally a DILM consists of a 50/50 coupler and a fiber loop made of one segment of high anomalous dispersion SMF, and another segment of dispersion-shifted fiber (DSF) or high nonlinear DSF (HNLF) with a much lower dispersion. The unique switching property of the DILM is that only pulses are switched

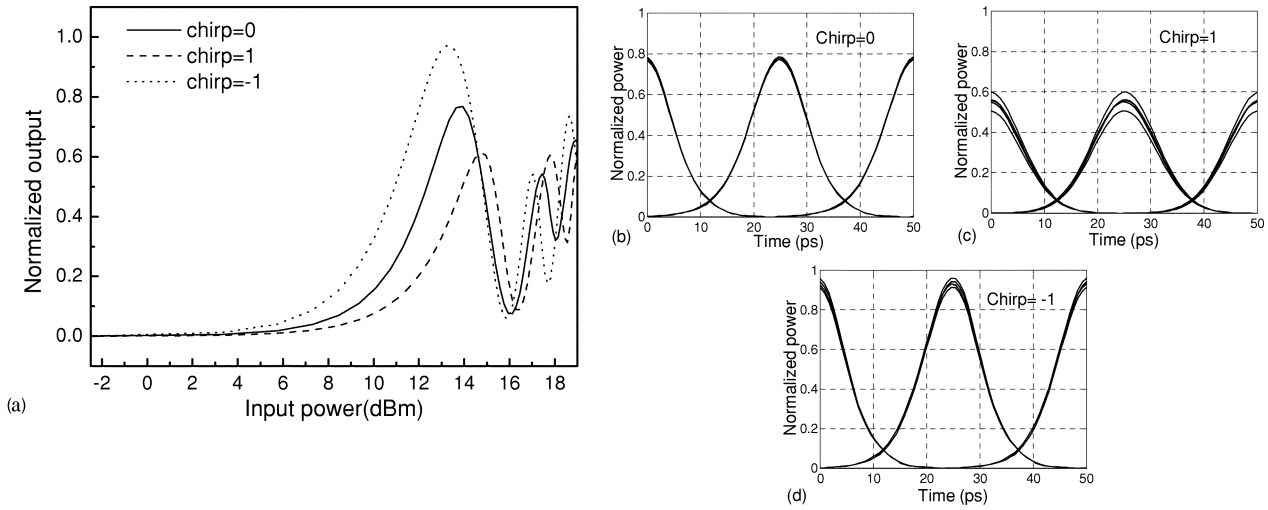

Fig. 4. Optical power transfer characteristics and output eye diagrams of a DILM for different initial chirp.

out whereas CW light of arbitrary intensity is totally reflected because dispersion only affects pulses [14]. When the noise-loaded signals enter the DILM, only the data signals have sufficient power to open the switching window whereas noise does not, so the data signals are reshaped by the DILM.

The quasiinstantaneous response of Kerr nonlinearity in fibers makes it a most attractive effect to overcome bandwidth limitations [2]. The DILM can be regarded as a NOLM where the symmetry of the loop is broken in a truly passive manner by making the dispersion of the fiber loop asymmetric [17]. When the signal light enters the DILM through one port of the 50/50 coupler, the incident light is split into two parts before it propagates in the fiber loop in two different directions. The pulse propagates in the SMF first, assuming it is the clockwise-propagating beam, disperses quickly and its peak power decreases as the pulsewidth broadens, so that in the second fiber segment it gets less nonlinear phase shift than the counter propagating beam. When the phase shift difference between these two beams equals π, the maximum transmission of the DILM occurs.

A. The Mach-Zehnder Interferometer Model and Optimum Fiber Length

Here, A_1 and A_2 are the amplitudes of the electric fields propagating in the two fiber arms; A_1 relates to propagation in first the SMF and then the HNLF, A_2 vice versa. The propagation of the fields in the fiber is governed by the coupled nonlinear Schrödinger equations

$$\frac{\partial A_i}{\partial z}+\frac{1}{V_{g,s}}\frac{\partial A_i}{\partial t}+i\frac{\beta_{2,s}}{2}\frac{\partial^2 A_i}{\partial t^2}+\frac{\beta_{3,s}}{6}\frac{\partial^3 A_i}{\partial t^3}=i\gamma_s\left|A_i\right|^2 A_i \tag{2}$$

$$\frac{\partial A_i}{\partial z}+\frac{1}{V_{g,h}}\frac{\partial A_i}{\partial t}+i\frac{\beta_{2,h}}{2}\frac{\partial^2 A_i}{\partial t^2}+\frac{\beta_{3,h}}{6}\frac{\partial^3 A_i}{\partial t^3}=i\gamma_h\left|A_i\right|^2 A_i. \tag{3}$$

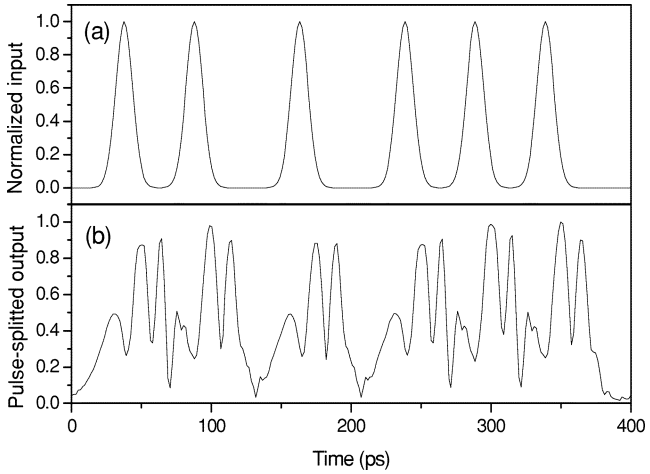

Fig. 5. (a) Input pulses versus time. (b) Distorted output pulses with a multipeak structure stemming from an input peak power that exceeds the optimum value.

Here, β_2 is the dispersion parameter, β_3 is the third-order dispersion, A_i ($i=1, 2$) denotes amplitudes of the electric fields in the two arms, the index s stands for SMF and h for HNLF. γ is the nonlinear coefficient defined as $2\pi n_2/\lambda A_{eff}$, n_2 the nonlinear refractive index of the fiber and A_{eff} the effective core area. V_g is the group velocity.

A fundamental performance of such a nonlinear device used in WDM systems is considered to come from the XPM between different channels. Since the magnitude of XPM is larger than that of self-phase modulation by a factor of two (of the worst case of polarization-matched signals), its effect cannot be neglected unless the walk-off time between the signals is very large. In particular, the XPM effect depends on the overall power in all the other channels and the channelling [18]–[20]. Thus, in the numerical analysis we assume a channel spacing of 200 GHz is wide enough to neglect the XPM effect, the following experiment also proves that the XPM effect could be negligible for the signals at 10 Gbit/s when the channel separation is 200 GHz.

Assuming the input pulses are Gaussian with a full width at half maximum (FWHM) of 5 ps, the bit rate is 40 Gb/s, the

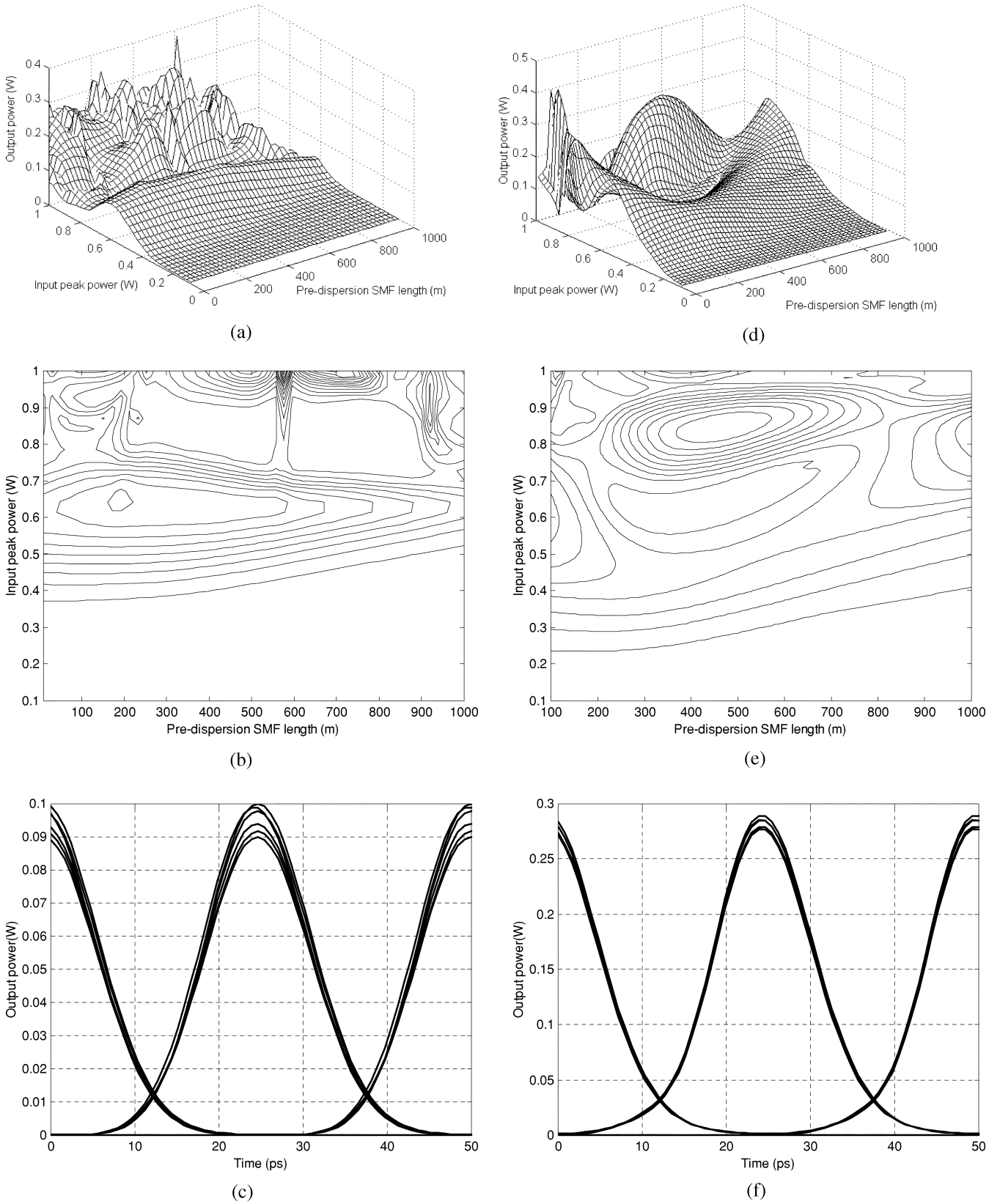

Fig. 6. (a) Three-dimensional and (b) contour plots of output power versus predispersion SMF length and input peak power for an input extinction ratio of 5 dB. (c) Output eye diagram at the optimum point of (b). (d) and (e) Similar plots for a larger input extinction ratio of 20 dB. (f) Output eye diagram at the optimum point of (e).

predispersion is equal to zero and the input peak power is 0.1 W, the output average power versus SMF length and HNLF length is shown in Fig. 2. From the contour plot the maximum transmission point can be easily seen. When the SMF length is in-

creased from 0.1 to 5 km, the output power first increases, and then decreases beyond the maximum transmission point. On the other hand, for the HNLF the output power exhibits two peaks as the HNLF length is increased. The first peak (on the left) shows the optimum fiber length for a certain input peak power. Though the second peak shows larger transmission than the first one, the nonlinear effect is too large and the output pulses is distorted. The position of the peak will change as a consequence of varying input peak power. Therefore, it can be concluded that there exists an optimized input peak power provided the lengths of the constituent fibers of a DILM are fixed; this optimized point can be reached by using an tunable attenuator.

The output extinction ratio versus input average power is shown in Fig. 3. Considerable enhancement in extinction ratio can be achieved after transmission through the DILM. When the input power increases, the output extinction raio first increases, and then decreases beyond the maximum transmission point. The output exinction ratio can be improved by 19 dB when an input extinction raio is 5 dB. And for an input extinction ratio at 10 dB, the maximum improvement of output extinction ratio is 16 dB.

B. Initial Chirp and Predispersion

Fig. 4. shows the normalized output versus input power for three different initial chirp values. For an SMF-HNLF DILM, negative initial chirp is preferred due to its larger output. This can be explained as follows. The pulse with negative initial chirp will rapidly broaden and the peak power of the pulse will decrease accordingly; this leads to an enhancement of the phase difference bringing it closer to π, hence larger transmission occurs. In practice, this initial chirp is generally provided by a segment of SMF fiber [16], so-called predispersion. If the input power exceeds 18 dBm, on the rising and trailing edges the pulse will experience some switching out at a certain power level and a multipeak structure is predicted as shown in Fig. 5 with the input bit sequence as 0 101 001 001 010 100. So the input power is a very critical parameter for a DILM.

As expected varying the predispersion length will cause the transmission function of the DILM to change (see Fig. 6). Optimized predispersion fiber length and input peak power can be obtained from the peak of the output power. The optimized input peak power for a low input extinction ratio is smaller than for a high input extinction ratio, which is in agreement with Fig. 3. Low input extinction ratio also requires a short predispersion fiber length.

C. WDM Operation

Because the switching mechanism of the DILM relies on the dispersion asymmetry of the fiber loop, the dispersion of the fibers will significantly influence transmission function. Thus for multichannel operation, the accumulated dispersion should be approximately constant in the operating wavelength range.

Assuming the predispersion length is fixed at 200 m, we increase the SMF fiber length in the DILM from 0.2 to 2.5 km to evaluate the output peak power of two wavelength channels

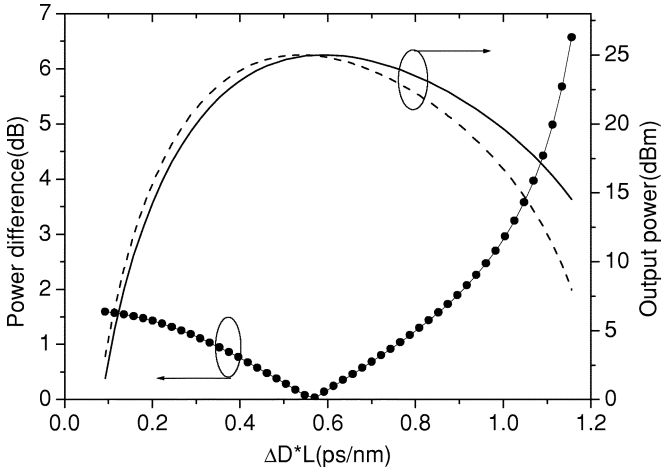

Fig. 7. Output peak power versus dispersion difference of two wavelength channels at 1540 nm (solid line) and 1560 nm (dotted line) respectively. Also their difference in peak power is plotted.

at 1540 and 1560 nm, respectively. Fig. 7 demonstrates that the power difference has a minimum value when the accumulated dispersion difference $\Delta D \cdot L$ is 0.56 ps/nm.

Moreover, simulation results for six channels at the ITU standard wavelengths (1549.3 nm, 1550.9 nm, 1552.5 nm, 1554.1 nm, 1555.7 nm and 1557.3 nm, respectively) are shown in Fig. 8. The predispersion length and the HNLF length are now fixed at 100 m and 3 km, respectively. The most flat output power can be obtained when the SMF length is 1500 m; below or above this length, not only the transmitted optical power will be reduced, but also the fluctuations between channels will increase.

Here we assume that the beams experience dispersion effect in the SMF and nonlinear effect in HNLF in order to deduce the expression for the power difference between channels. Considering two input signals, which has the same input peak power and same pulsewidth but different wavelengths, the peak power after transmission in the SMF is given by

$$P_i = \frac{1}{\sqrt{1+\frac{L_s^2\beta_{2i}^2}{T_0^4}}} P_0 \tag{4}$$

where P_0 is the incident optical power and index i ($i = 1, 2$) denotes different channels. L_s is the SMF length and T_0 the half-width of the pulse at $1/e$-intensity point. The output power of the DILM is given by

$$P_{\text{out,i}} = \frac{P_0}{2}\left\{1-\cos\left[\gamma P_0 L_h\left(1-\frac{1}{\sqrt{1+\frac{L_s^2\beta_{2i}^2}{T_0^4}}}\right)\right]\right\} \tag{5}$$

where γ is the nonlinear coefficient of the HNLF and L_h is the length of the HNLF.

By using $\beta_2 = -(D\lambda^2)/(2\pi c)$ and $D_2 = D_1 + (\lambda_2 - \lambda_1)S$, where D is the dispersion parameter, λ is the wavelength, c is

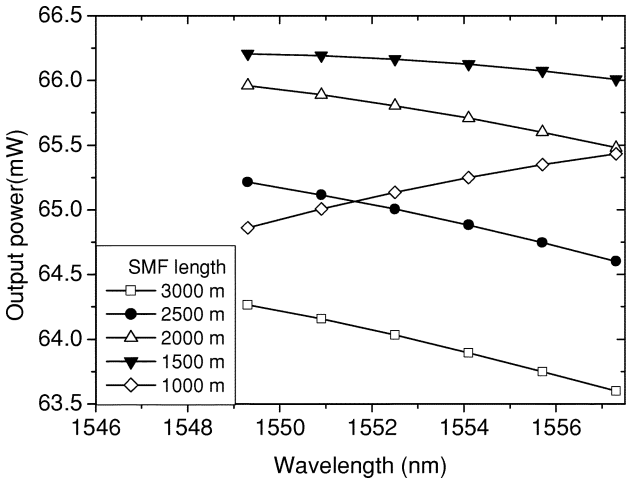

Fig. 8. Output power of six WDM channels versus wavelength for five different SMF lengths in the DILM.

the speed of light, and S is the dispersion slope, the power difference is given by (see Appendix)

$$\Delta P_{\text{out}} = P_0 \sin\left(\frac{\gamma P_0 L_h L_s^2 \lambda_1^4 D_1 S(\lambda_2 - \lambda_1)}{8\pi^2 c^2 T_0^4}\right). \quad (6)$$

Assuming the nonlinear phase shift of channel 1 is equal to π, which could be realized by adjusting the polarization controller [21], the normalized power difference assumes the simple expression

$$\Delta P_{\text{out}} = P_0 \sin\left(\frac{2\pi S(\lambda_2 - \lambda_1)}{D_1}\right). \quad (7)$$

If the power difference between these two channels should be smaller than 3 dB, the accumulated dispersion and slope should satisfy

$$12S(\lambda_2 - \lambda_1) < D_1. \quad (8)$$

III. Experimental Results

The experimental setup is shown in Fig. 9. The six-channel RZ pulses are realized by using wavelength conversion in a nonlinear optical loop mirror (NOLM). The NOLM consists of 3-km DSF that has zero dispersion at 1554.7 nm with a dispersion slope of 0.08 ps/nm/km. The control signal is generated by a 10 GHz, 1559 nm erbium fiber ring laser (ERFL) with a FWHM of 4.1 ps. After the $LiNbO_3$ modulator the pulse is modulated by a pseudorandom bit sequence of $2^{31}-1$. In order to get sufficient XPM effect in the NOLM the control signal is amplified to an average power of 18 dBm. A 2-nm band-pass filter is used after the EDFA to suppress the ASE noise and to broaden the pulsewidth to 6.9 ps because walk-off effect will do more harm to narrower pulses. Then the control signal is coupled into the loop by a 50/50 coupler. A tunable attenuator is used to obtain optimum control power. The probe CW light beams are provided by six distributed feedback (DFB) lasers combined in a WDM multiplexer with a frequency spacing of 200 GHz. The wavelengths of these

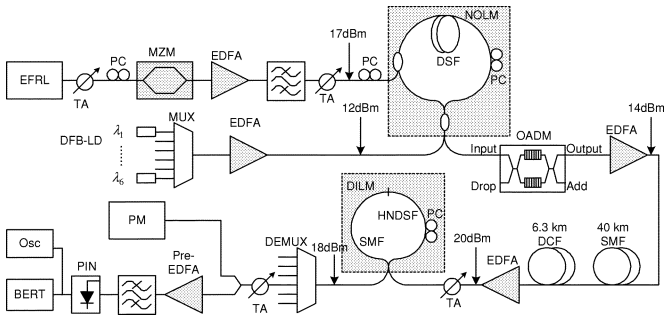

Fig. 9. Experimental setup. ERFL: erbium fiber ring laser, PC: polarization controller, MZM: Mach-Zehnder modulator, MUX: WDM multiplexer, DEMUX: WDM demultiplexer, TA: tunable attenuator, PM: power meter, Osc: oscilloscope.

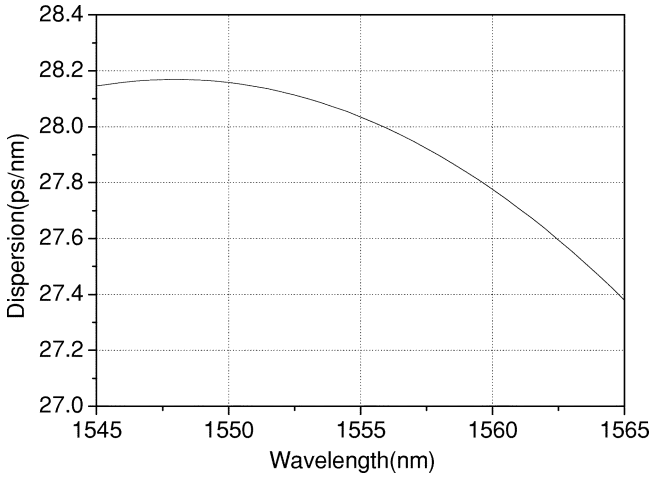

Fig. 10. Accumulated dispersion of 40-km SMF plus 6.3 km DCF plus 1.03 km SMF.

lasers are 1549.3 nm, 1550.9 nm, 1552.5 nm, 1554.1 nm, 1555.7 nm, and 1557.3 nm, respectively, in compliance with the ITU-standardized wavelength proposal. A 1559-nm optical add-drop multiplexer (OADM) acting as an optical notch filter at the output of the NOLM is used to suppress the control pulses before the WDM signals are amplified and transmitted.

After transmission over a fiber span consisting of 40-km conventional SMF and 6331 m DCF, the transmitted signals are then reamplified and put into the DILM to be reshaped. The DILM, constructed from a 50/50 coupler and 1030 m of SMF and 1 km HNLF, acts as a nonlinear filter that transmits only pulse components with appropriate peak power and pulse duration. The newly developed HNLF has a high nonlinear coefficient $\gamma = 10.6\,\text{W}^{-1}\text{km}^{-1}$. This is achieved by a high-index Germanium-doped core and deeply depressed ring, reducing the effective area to $\sim 12\ \mu\text{m}^2$. The zero dispersion wavelength of the HNLF is at 1553.6 nm and the dispersion slope is 0.022 ps/nm/km.

The SMF length in the DILM must be carefully designed so that the total dispersion accumulated over the 40-km fiber as well as over the SMF in the DILM could be approximately constant in the operating wavelength range. Fig. 10 shows the accumulated dispersion curve of the 40 km SMF plus the 6.3 km DCF, and 1.03 km SMF in the DILM. The differences in accumulated dispersion among the six wavelengths are within

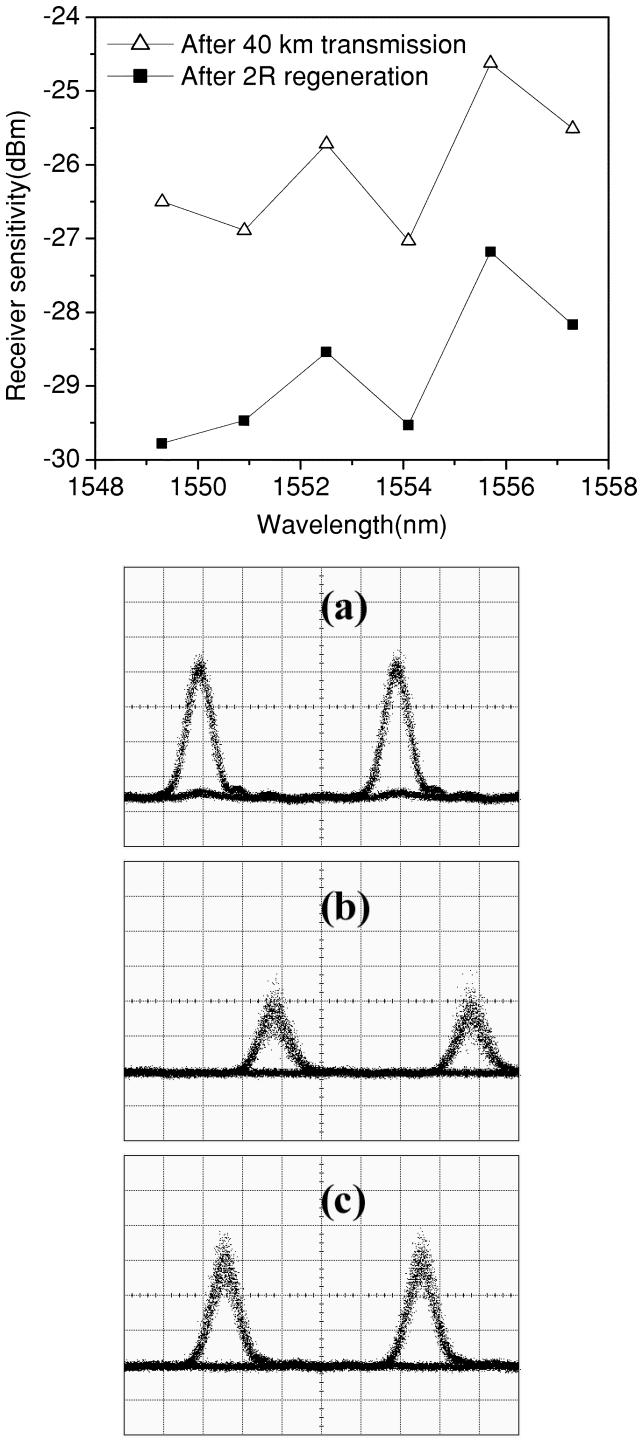

Fig. 11. Receiver sensitivity versus wavelength of the six WDM signals and eye diagrams of (a) control signal. (b) Channel 5 after 40 km transmission. (c) Channel 5 after regeneration.

0.8 ps/nm, which guarantees the multiwavelength operation of the DILM.

After 2R regeneration, the receiver sensitivity of the six-channel WDM signals are measured when the BER is below 10^{-9} (see Fig. 11). The eye diagram tested by a 30-GHz photodiode indicates a clear eye opening. Channel 5 (1555.7 nm) shows the largest penalty of more than 6 dB after wavelength conversion and 40 km transmission because of the largest walk-off. The receiver sensitivity is improved by 2.5–3.3 dB after the regeneration. The fluctuation of the receiver sensitivity between the six wavelengths is within 2.6 dB.

IV. Conclusion

In this paper, a detailed study of a DILM has been reported. In particular, a Mach-Zehnder interferometer has been considered as an equivalent to the Sagnac loop mirror. Based on this model and coupled Schrödinger equations, transfer function, output extinction ratio, and predispersion fiber length have been investigated. Moreover, the WDM transfer characteristics of the DILM have been numerically simulated and the results predict the possibility that the DILM can work as a WDM 2R regenerator.

It is concluded that the input peak power is a critical parameter to achieve good transfer function and output extinction ratio. Hence, in practice, a tunable attenuator is indispensable to adjust the input power to the optimum level. Though signals may have some residual dispersion after transmission due to insufficient compensation of dispersion and dispersion slope, this residual dispersion can be treated as predispersion outside the loop and theoretical analysis shows certain predispersion can benefit the transfer function.

The principle of a DILM is based on dispersion effect, thus use of the DILM as a WDM regenerator will limit the allowable dispersion difference between WDM channels. If the accumulated fiber dispersion and dispersion slope satisfies $12S(\lambda_2 - \lambda_1) < D_1$, the output power difference between channels will less than 3 dB.

In DILMs, the phase difference must approach π in order to achieve 100% power transmission. The input power must therefore be in the 50–100 mW range, which is well above the stimulated Brillouin scattering (SBS) threshold. As SBS induces nonlinear loss in the signal power, low switching efficiency and increased insertion loss result in the DILM. It can be observed in the experiments that SBS is also a source of device instability. SBS suppression techniques must therefore be considered in the design of the DILM.

It can be envisaged that XPM will not be negligible when using such devices in dense WDM system with narrower channelling and higher speed. Moreover, in our experiment the WDM channels are not decorrelated. Therefore to make full demonstration, future experiment would be required by using well-decorrelated WDM signals for higher speed operation with narrower channel separations at the DI-NOLM.

Our multichannel experiment shows the receiver sensitivity is increased by around 3 dB by the 2R regenerator, which proves that the DILM can be used as WDM 2R regenerator. However, the WDM signals after wavelength conversion and 40 km transmission have different power levels due to the walk-off in the NOLM that acts as a wavelength converter. This initial input power difference makes it difficult to evaluate the flatness of the transfer function of the DILM. Also because of the absence of SBS suppression, SBS becomes a severe limitation for achieving better receiver sensitivity. It can be predicted that the improvement in receiver sensitivity would be larger than 3 dB if appropriate SBS suppression had been used.

APPENDIX

The output power difference between the two channels is

$$
\begin{aligned}
&P_{\text{out},1} - P_{\text{out},2} \\
&= \frac{P_0}{2}\left\{\cos\left[\gamma P_0 L_h\left(1 - \frac{1}{\sqrt{1+\frac{L_s^2\beta_{21}^2}{T_0^4}}}\right)\right]\right. \\
&\quad \left. - \cos\left[\gamma P_0 L_h\left(1 - \frac{1}{\sqrt{1+\frac{L_s^2\beta_{22}^2}{T_0^4}}}\right)\right]\right\} \\
&= P_0 \sin\left[\gamma P_0 L_h\left(1 - \frac{1}{2\sqrt{1+\frac{L_s^2\beta_{21}^2}{T_0^4}}} - \frac{1}{2\sqrt{1+\frac{L_s^2\beta_{22}^2}{T_0^4}}}\right)\right] \\
&\quad \cdot \sin\left[\gamma P_0 L_h\left(\frac{1}{\sqrt{1+\frac{L_s^2\beta_{22}^2}{T_0^4}}} - \frac{1}{\sqrt{1+\frac{L_s^2\beta_{21}^2}{T_0^4}}}\right)\right].
\end{aligned}
$$

Given the nonlinear phase difference between the two channels is less than $\pi/6$, the first sine function is larger than 0.97 and approximately equal to 1; hence, we get

$$
\begin{aligned}
P_{\text{out},1} - P_{\text{out},2} &\approx P_0 \sin\left[\frac{\gamma P_0 L_h}{2}\left(\frac{L_s^2\beta_{22}^2}{2T_0^4} - \frac{L_s^2\beta_{21}^2}{2T_0^4}\right)\right] \\
&= P_0 \sin\left[\frac{\gamma P_0 L_h L_s^2}{16\pi^2 c^2 T_0^4}\left(D_2^2\lambda_2^4 - D_1^2\lambda_1^4\right)\right].
\end{aligned}
$$

Using $D_2 = D_1 + (\lambda_2 - \lambda_1)S$ and neglecting the component which proportional to higher order of $\lambda_2 - \lambda_1$, the result then becomes

$$
P_{\text{out},1} - P_{\text{out},2} \approx P_0 \sin\left(\frac{\gamma P_0 L_h L_s^2 \lambda_1^4 D_1 S(\lambda_2 - \lambda_1)}{8\pi^2 c^2 T_0^4}\right)
$$

ACKNOWLEDGMENT

The authors would like to thank S. N. Knudsen at OFS Fitel I/S for having supplied the highly nonlinear fiber.

REFERENCES

[1] B. Sartorius, "3R regeneration for all-optical networks," in *Proc. 2001 3rd Int. Conf. Transparent Opt. Networks*, 2001, Th.A4, pp. 333–337.

[2] S. Bigo, O. Leclerc, and E. Desurvire, "All-optical fiber signal processing and regeneration for soliton communications," *IEEE J. Select. Topics Quantum Electron.*, vol. 3, pp. 1208–1223, 1997.

[3] O. Brox, A. Kilk, C. Caspar, D. Hoffmann, M. Mohrle, G. Sahin, and B. Sartorious, "Q-switched laser module for regenerative wavelength conversion," in *Proc. Eur. Conf. Opt. Commun. (ECOC'2000)*, vol. 2, 2000, pp. 57–58.

[4] T. Otani, T. Miyzaki, and S. Yamamoto, "40 Gb/s signal transmission using optical 3R regenerator based on electroabsorption modulators," in *Proc. Opt. Commun. Conf. (OFC'2000)*, vol. 4, 2000, pp. 226–227.

[5] D. wolfson, A. Kloch, T. Fjelde, C. Janz, B. Dagens, and M. Renaud, "40-Gb/s all-optical wavelength conversion, regeneration, and demultiplexing in an SOA-based all-active Mach-Zehnder interferometer," *IEEE Photon. Technol. Lett.*, vol. 12, pp. 332–334, 2000.

[6] Y. Ueno, S. Nakamura, and K. Tajima, "Penalty-free error-free all-optical data pulse regeneration at 84 Gb/s by using a symmetric-Mach-Zehnder-type semiconductor regenerator," *IEEE Photon. Technol. Lett.*, vol. 13, pp. 469–471, 2001.

[7] S. Boscolo, S. K. Turitsyn, and K. J. Blow, "All-optical passive regeneration of 40 Gbit/s soliton data stream using dispersion management and in-line nonlinear optical loop mirrors," in *OFC'2001*, vol. 1, 2001, MF6.

[8] ——, "All-optical passive regeneration of 40 Gbit/s soliton data stream using dispersion management and in-line NOLM's," *Electron. Lett.*, vol. 37, pp. 112–113, 2001.

[9] ——, "Study of the operating regime for all-optical passive 2R regeneration of dispersion-managed RZ data at 40 Gbit/s using in-line NOLM's," *IEEE Photon. Technol. Lett.*, vol. 14, pp. 30–32, 2002.

[10] K. R. Tamura and M. Nakazawa, "A polarization-maintaining pedestal-free femtosecond pulse compressor incorporating an ultrafast dispersion-imbalanced nonlinear optical loop mirror," *IEEE Photon. Technol. Lett.*, vol. 13, pp. 526–528, 2001.

[11] I. Y. Khrushchev, "Picosecond pulse source for OTDM/WDM applications based on arrayed waveguide grating," in *OFC'99*, 1999, ThT5, pp. 296–298.

[12] ——, "OTDM applications of dispersion-imbalanced fiber loop mirror," *Electron. Lett.*, vol. 35, no. 14, pp. 1183–1185, 1999.

[13] W. S. Wong, "In-band amplified spontaneous emission noise filtering with a dispersion -imbalanced nonlinear loop mirror," *J. Lightwave Technol.*, vol. 16, pp. 1768–1772, 1998.

[14] ——, "Self-switching of optical pulses in dispersion-imbalanced nonlinear loop mirrors," *Opt. Lett.*, vol. 22, no. 15, pp. 1150–1152, 1997.

[15] N. Chi, S. Chen, L. Xu, J. Qi, Y. Qiao, and Y. Zheng, "A new scheme of cross-gain modulation wavelength converter with good performance on extinction ratio," *Opt. Commun.*, vol. 189/4–6, pp. 235–239, 2001.

[16] M. Matsumoto and T. Ohishi, "Dispersion-imbalanced nonlinear optical loop mirror with lumped dispersive elements," *Electron. Lett.*, vol. 34, no. 11, pp. 1140–1141, 1998.

[17] A. L. Steele, "Pulse compression by an optical fiber loop mirror constructed from two different fibers," *Electron. Lett.*, vol. 29, no. 22, pp. 1971–1972, 1993.

[18] S. Betti and M. Giaconi, "Analysis of the cross-phase modulation effect in WDM optical systems," *IEEE Photon. Technol. Lett.*, vol. 13, Jan. 2001 AU; PLS UPDATE PP#'s—Ed.

[19] M. S. Shtaif, "Analytical description of cross-phase modulation in dispersive optical fibers," *Opt. Lett.*, vol. 23, no. 15, pp. 1191–1193, Aug. 1998.

[20] M. Shtaif and M. Eiselt, "Analysis of intensity interference caused by cross-phase modulation in dispersive optical fibers," *IEEE Photon.Technol. Lett.*, vol. 10, pp. 979–981, July 1998.

[21] C. Kolleck and U. Hempelmann, "All-optical wavelength conversion of NRZ and RZ signals using a nonlinear optical loop mirror," *J. Lightwave Technol.*, vol. 15, pp. 1906–1913, 1997.

Nan Chi was born in Liaoning, China, on March 3, 1974. She received the B.S. and Ph.D. degrees in electrical engineering from Beijing University of Posts and Telecommunications, Beijing, China, in 1996 and 2001, respectively.

Since 2001, she has been an Assistant Professor with the Research Center COM, Technical University of Denmark, Lyngby. Her research interests are in the area of optical packet switching, all-optical processing, and optical labeling.

Birger Carlsson, photograph and biography not available at the time of publication.

Palle Jeppesen (M'69) was born in Vordingborg, Denmark, on August 6, 1941. He received the M.Sc., Ph.D., and Dr. Sc. degrees in electrical engineering from the Technical University of Denmark, Lyngby, in 1967, 1970, and 1978, respectively.

He was a Research Associate at Cornell University, Ithaca, NY, from 1968 to 1969 and a Project Engineer at Cayuga Associates, Ithaca, NY, from 1969 to 1970; in both positions, he conducted research on GaAs Gunn-effect microwave oscillators. From 1970 to 1998, he was an Assistant, Associate, Research, and Full Professor at EMI, Technical University of Denmark, first in microwave electronics, and, since 1974, in optical communications. At EMI, he was Head of Optogroup from 1974 to 1988 and Head of the Center for Broadband Telecommunications from 1988 to 1998. From 1982 to 1984, he also worked as part-time Manager of Reasearch and Development at NKT Elektronik, now Draka Denmark Optical Cable, OFS Fitel Denmark, and Tellabs Denmark. From 1995 to 1998, he coordinated the participation of the Technical University of Denmark in the EU ACTS project METON (METropolitan Optical Network). Since 1999, he has been Professor in optical communications at Research Center COM, Technical University of Denmark, where he is heading the systems competence area. His current research interests are high-speed WDM optical communication systems, dispersion maps, WDM devices, and optical signal processing.

Dr. Jeppesen has been a Member of the NATO Research and Technology Board since 1997 and the NATO Science Committee since 1999. He was Chairman of the European Conference on Optical Communication (ECOC) in 1981 and 2002. He received the P.Gorm Petersens Memorial Stipend in 1974, the Esso-prize in 1978, and the Villum Kann Rasmussen Prize in 1988.